Dielectric properties in A-site substitution type relaxor ferroelectric perovskite titanates $Ba_{1-x}(La_{0.5}Na_{0.5})_xTiO_3$

2002 J. Phys.: Condens. Matter 14 2043

(http://iopscience.iop.org/0953-8984/14/8/330)

INSTITUTE OF PHYSICS PUBLISHING JOURNAL OF PHYSICS: CONDENSED MATTER

J. Phys.: Condens. Matter **14** (2002) 2043–2051 PII: S0953-8984(02)28471-4

Dielectric properties in A-site substitution type relaxor ferroelectric perovskite titanates $Ba_{1-x}(La_{0.5}Na_{0.5})_xTiO_3$

S Komine and E Iguchi[1]

Division of Materials Science and Engineering, Graduate School of Engineering, Yokohama National University, Tokiwadai, Hodogaya-Ku, Yokohama, 240-8501, Japan

E-mail: iguchi@post.me.ynu.ac.jp

Received 3 September 2001, in final form 10 January 2002
Published 15 February 2002
Online at stacks.iop.org/JPhysCM/14/2043

Abstract

In order to investigate the effect of A-site substitution on phase transitions in barium titanates, dielectric permittivity in $Ba_{1-x}(La_{0.5}Na_{0.5})_xTiO_3$ was measured in the temperature range up to 400 K with frequency of 100 Hz to 100 kHz by changing x from 1/8 to 4/8. The transition from classical non-relaxor ferroelectric ($x = 1/8$) to relaxor ferroelectric ($x \geqslant 3/8$) occurs, through the intermediate between classical non-relaxor and relaxor ferroelectrics ($x = 2/8$). There is a strong correlation between the ionic mass at the A site M and the temperature of the permittivity maximum. It is found that M is one of the important parameters which dominates the dielectric permittivity and phase transitions in perovskite titanates. The diffusive displacement of Ti^{4+} due to the random fields created by inhomogeneity which A-site substitution introduces, besides the displacement suppressed by the shrinkage of lattice constant, reduces the permittivity maximum when $x \geqslant 3/8$.

1. Introduction

$BaTiO_3$, one of the displacive-type ferroelectric materials, is a typical ABO_3-type simple perovskite oxide. Substitution of other ions for host cations at the A or B site in $BaTiO_3$ leads to remarkable changes in various characteristics [1–3]. In non-conductive perovskite ABO_3, B-site substitution is well known to bring about the classical non-relaxor–relaxor ferroelectric transition [4–6]. $BaTi_{1-x}Zr_xO_3$ (BZT), a new lead-free relaxor ferroelectric, attracts attention from the viewpoint of environmental preservation [7]. This BZT system has predominantly three different phases, classical ferroelectric $BaTiO_3$ at $x = 0$, antiferroelectric $BaZrO_3$ at $x = 1$ and relaxor ferroelectric BZT around $x = 0.35$. The random potential in the lattice created by the disordered distribution of Ti^{4+} and Zr^{4+} at the B site is indispensable for describing the physics of BZT.

[1] Author to whom any correspondence should be addressed.

In a relaxor ferroelectric, there is one broad peak in real and imaginary permittivity, ε_r' and ε_r'', and frequency dispersion takes place, i.e. an increase of T_m and a decrease of ε_r' with increasing frequency, where T_m is the temperature of the dielectric permittivity maximum. In the prototypical relaxor $PbMg_{1/3}Nb_{2/3}O_3$, the disordered distribution of B-site cations plays an important role in the classical non-relaxor–relaxor transition just like the BZT system [4,8]. The origin of the relaxor is a dynamic polar cluster created by the disordered distribution of B-site cations [9–12].

Not only B-site substitution but also A-site substitution is very important. $Ln_{0.5}Na_{0.5}TiO_3$ (Ln, lanthanide) [13, 14] is ferroelectric at $M > M_0$, while quantum paraelectric at $M < M_0$, where M is the ionic mass at the A site and M_0 is 100 au, which is close to the mass of TiO_3 (95.9 au) [15]. The ionic mass at the A site governs this paraelectric–ferroelectric transition because the A-site cation is one end of the two-particle simple harmonic oscillator, and M_0 is the critical value in this transition. In BZT where Ba^{2+} ions at the A site are partially replaced with Ca^{2+}, the characteristic of the relaxor becomes more remarkable by the assistance of the random potential due to Ca^{2+} substitution at the A site overlapping with the potential created by $Ti_{1-x}Zr_x$ at the B site [16, 17]. Even A-site-substituted quantum paraelectric $Sr_{1-x}Ca_xTiO_3$ exhibits behaviour similar to a relaxor when x is very small [18,19]. The effect of the A-site cation should then be investigated in the research on relaxors. Variations of ionic radius, mass and charge of the A-site cation would provide very useful knowledge in the elucidation of the A-site effect in non-conductive perovskite titanates.

It is then of great importance to investigate the correlation between the substitution effect at the A sites and dielectric properties in $ATiO_3$ so as to clarify the transition mechanism peculiar to perovskite titanates, and also to develop new compounds with high permittivities from the viewpoint of practical application. From this point of view, this study has prepared specimens of $Ba_{1-x}(La_{0.5}Na_{0.5})_xTiO_3$ ($x = 1/8$–$4/8$). Since Ba^{2+}, La^{3+} and Na^+ have different ionic radii, masses and electronic charges, the relationship of the phase transition and A-site substitution would be possible to elucidate as a parametric function of x in $Ba_{1-x}(La_{0.5}Na_{0.5})_xTiO_3$. In particular, this study concentrates on the ionic mass at the A site and the random potential created by A-site substitutions because these are the most important parameters which dominate directly the substitution effect at the A site.

2. Sample preparation

$Ba_{1-x}(La_{0.5}Na_{0.5})_xTiO_3$ ($x = 1/8$, $2/8$, $3/8$ and $4/8$) polycrystalline ceramic specimens were prepared by a conventional standard solid-state synthesis technique [7]. $BaCO_3$ (3 N), La_2O_3 (4 N), Na_2CO_3 (3 N) and TiO_2 (3 N) powders were used. In order to evaporate H_2O, La_2O_3 and Na_2CO_3 were preheated at 1000 °C for 10 h and 600 °C for 1 h before weighing. The appropriate mixtures of these powders were calcined in flowing pure oxygen at 1100 °C for 12 h, and then, after mixing very carefully, calcined again in the same conditions. The powders were then pressed into pellets, and finally sintered in flowing pure oxygen at 1300 °C for 5 h. As for the specimen $x = 1/8$, however, the calcining and sintering temperatures were 1200 and 1350 °C. The temperatures employed here are rather low in comparison with the preparation of $BaTiO_3$ and this is to suppress a deficit of sodium [13]. Furthermore, sodium was weighed 5 wt% extra.

3. XRD studies

All of the sintered specimens were analysed, using an x-ray diffractometer (XRD) with Cu Kα radiation with step scanning at room temperature. Figure 1 demonstrates the XRD patterns

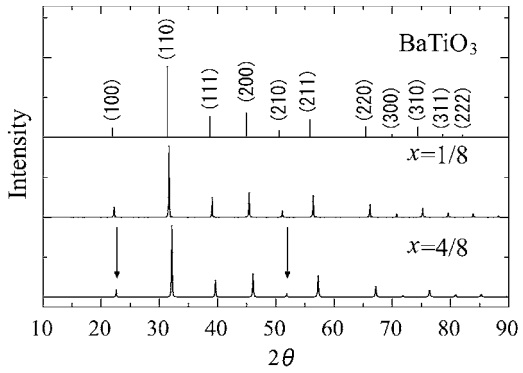

Figure 1. The XRD patterns of $Ba_{1-x}(La_{0.5}Na_{0.5})_xTiO_3$ ($x = 1/8$ and $4/8$) and cubic $BaTiO_3$ (JCPDS code 31-0174).

Table 1. Lattice constant based upon cubic perovskite a_p at room temperature, average ionic radius and average mass M at the A site for x in $Ba_{1-x}(La_{0.5}Na_{0.5})_xTiO_3$.

x	a_p (Å)	Radius (Å)	M (au)
0/8[a]	4.009	1.420	137.3
1/8	3.994	1.388	130.3
2/8	3.973	1.355	123.2
3/8	3.948	1.323	116.2
4/8	3.935	1.290	109.1
8/8[b]	3.873	1.170	80.95

[a] Tetragonal $BaTiO_3$.
[b] $La_{0.5}Na_{0.5}TiO_3$ [15].

at the compositions $x = 1/8$ and $4/8$, and that of cubic $BaTiO_3$ at $T \geqslant 408$ K with Miller indices. Even if x increases to $4/8$, the XRD pattern is substantially the same as that of cubic $BaTiO_3$, but the peak intensities at $2\theta \cong 22^\circ$ and 51° corresponding to (100) and (210) reduce to about 0.6 and 0.4. It should be noted that these peaks are very weak and barely observable at $x = 1$ ($La_{0.5}Na_{0.5}TiO_3$) [13, 20]. There are no patterns due to the ordered distribution of La^{3+}, Ba^{2+} and Na^+ ions at the A site. Table 1 tabulates the lattice constant, the average ionic radius and the mass at the A site for each x, where the estimation of the lattice constant is based upon cubic perovskite structure and Shannon's eight-coordination ionic radius [21] is employed in calculating the average ionic radius. Every parameter in table 1 decreases linearly with x and there is also a linear relation of the lattice constant and the average ionic radius at the A site, i.e. a reduction of the lattice constant with a decrease in the ionic radius.

4. Dielectric studies and discussion

The specimens for ac measurements were square discs of $5 \times 5 \times 1$ mm^3 and were polished by diamond paste. The square faces were evaporated with gold for an electrode. The values of ε_r' and ε_r'' were measured as a parametric function of frequency in the temperature range of 80–400 K for $x = 1/8$–$3/8$, and in the range of 10–400 K for $x = 4/8$ with heating rate 2 K min^{-1}, using an HP4284 LCR meter. A frequency of 100–100 kHz was employed. The permittivity behaviour observed in the present system is found to be very different from that of a classical ferroelectric such as $BaTiO_3$ or a quantum paraelectric such as $La_{0.5}Na_{0.5}TiO_3$.

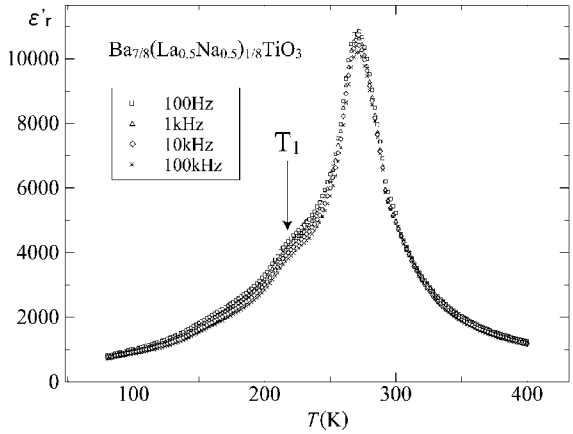

Figure 2. Temperature and frequency dependence of ε'_r for $x = 1/8$.

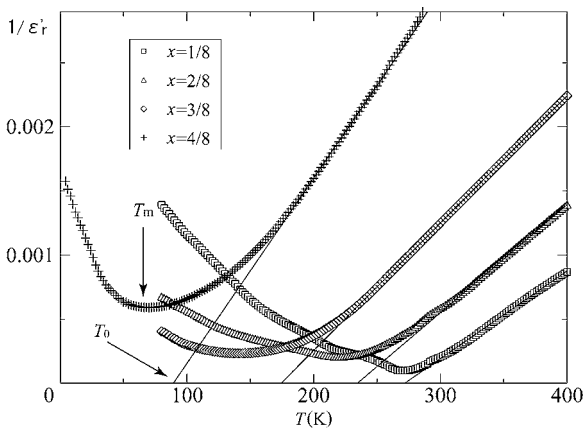

Figure 3. Temperature dependence of $1/\varepsilon'_r$ for all compounds. T_0 is the Curie temperature and T_m is the temperature of the dielectric permittivity maximum for $x = 4/8$.

4.1. Classical ferroelectric at $x = 1/8$

Figure 2 shows the temperature and frequency dependence of ε'_r for $x = 1/8$. Two of the three anomalies related to the phase transitions (rhombohedral–orthorhombic–tetragonal–cubic) for $BaTiO_3$ have been observed at $T_m \cong 270$ K and $T_1 \cong 230$ K. The anomaly at T_1 is very weak compared with the main peak at T_m. The values of T_m and T_1 were independent of frequency, implying this compound to be of approximately classical ferroelectric type. A very slight decrease of ε'_r occurs around T_1, indicating a weak component of relaxor involved in this compound.

Figure 3 depicts the variation of $1/\varepsilon'_r$ against T at 100 kHz. The Curie–Weiss relation, $\varepsilon'_r = C/(T - T_0)$, holds at $T \geqslant 270$ K where C is the Curie constant and T_0 is the Curie temperature. The experimental value for T_0 was nearly equal to T_m. In Landau's theory of phase transitions [17], a first-order transition takes place when $T_m > T_0$, and a second order in the case of $T_m = T_0$. For the composition $x = 1/8$, therefore, the second-order ferroelectric–paraelectric transition occurs as well as for BZT in which the composition is very close to $BaTiO_3$ [16, 17]. Speculation like this encourages the deduction that this oxide is a classical non-relaxor ferroelectric.

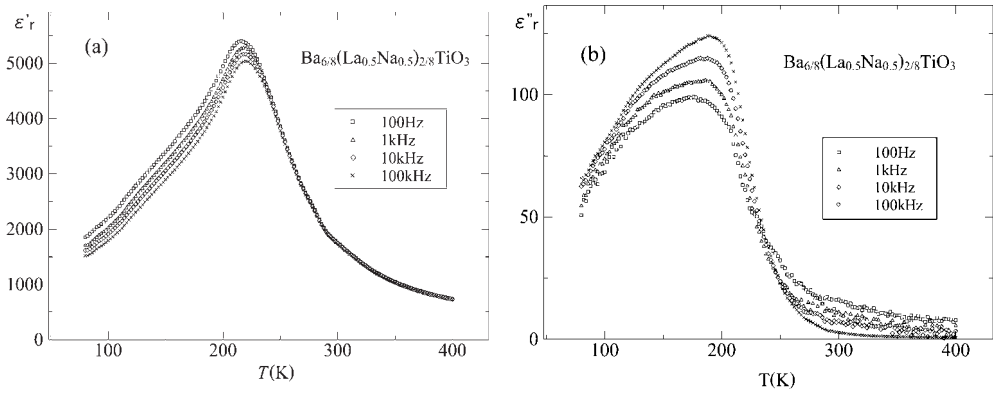

Figure 4. Temperature and frequency dependence of ε_r' (*a*) and ε_r'' (*b*) for $x = 2/8$.

4.2. Intermediate between non-relaxor and relaxor ferroelectric at $x = 2/8$

As well as the composition $x = 1/8$, two anomalies show up in the permittivity, i.e. the predominant one around 220 K and the very weak one around 130 K, as shown in figure 4. At the composition of $x = 2/8$, the Curie–Weiss relation holds and T_m at 100 kHz is lower than T_0 by approximately 10 K, as shown in figure 3. Furthermore, T_m is dependent upon the applied frequency (see figure 4). Because of these behaviours, the dielectric properties at $x = 2/8$ are different from those in not only the compound with $x = 1/8$ but also $BaTiO_3$. As for the weak anomaly around 130 K, the present study cannot obtain any direct evidence that clarifies the reason for this phenomenon.

Since the frequency dispersion is rather remarkable at $x = 2/8$, this composition is predominantly of relaxor ferroelectric type. However, some component of classical ferroelectric must be involved because of the weak anomaly around 130 K. Therefore, this compound must be intermediate between classical non-relaxor ferroelectric and relaxor ferroelectric.

4.3. Relaxor ferroelectric at $x \geqslant 3/8$

The compounds at $x = 3/8$ and $4/8$ contain a feature intrinsic to relaxor ferroelectric. Figures 5 and 6 exhibit the obvious frequency dispersion and there is no weak anomaly which occurs at a temperature lower than T_m when $x \leqslant 2/8$. Furthermore, T_m is lower than T_0 by 40 K or more, where T_0 is estimated using the Curie–Weiss relation in figure 3.

$\Delta\varepsilon/\varepsilon_r'$ and ΔT_m are the measures describing the character of a relaxor ferroelectric. In this report, $\Delta T_m = (T_m \text{ at } 100\text{ kHz}) - (T_m \text{ at } 100\text{ Hz})$, and $\Delta\varepsilon/\varepsilon_r' = [\varepsilon_r'(100\text{ Hz}) - \varepsilon_r'(100\text{ kHz})]/\varepsilon_r'(100\text{ Hz})$ at each temperature, $\varepsilon_r'(100\text{ Hz})$ and $\varepsilon_r'(100\text{ kHz})$ being ε_r' at 100 Hz and 100 kHz. Figure 7 illustrates the relation of $\Delta\varepsilon/\varepsilon_r'$ and T for $x = 3/8$. As temperature decreases from 400 K, $\Delta\varepsilon/\varepsilon_r'$ increases very slightly, but there is the onset of a rapid increase at 130–140 K, i.e. the temperature region of T_m [7]. ΔT_m is approximately 10 K at $x \geqslant 3/8$, about 3 K at $x = 2/8$ and nearly 0 K at $x = 1/8$. This was expected because the frequency dispersion becomes more remarkable when x is large.

The inset in figure 7 plots ε_r' and ε_r'' at 100 and 300 K against frequency. At 100 K, lower than T_m, there is a decrease in ε_r' and an increase in ε_r'' with frequency. At 300 K, higher than T_m, both ε_r' and ε_r'' are independent of frequency [7].

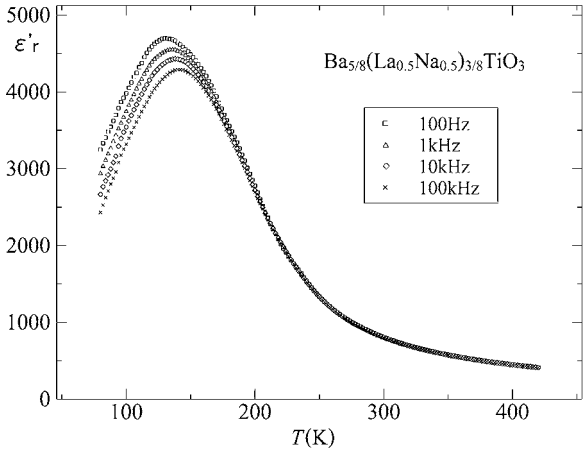

Figure 5. Temperature and frequency dependence of ε'_r for $x = 3/8$.

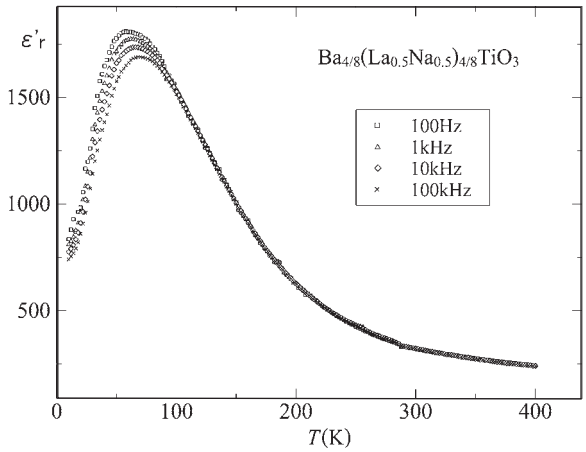

Figure 6. Temperature and frequency dependence of ε'_r for $x = 4/8$.

Materials of relaxor ferroelectric type are generally subject to the Vögel–Fulcher relation, which has the form $f = f_0 \exp[-E_a/(T_m - T_f)]$, where f, E_a and T_f are the applied frequency, the activation energy and the freezing temperature with a constant f_0. The compounds with $x = 3/8$ and $4/8$ are also subject to this relation. As for $x = 3/8$, E_a and T_f are estimated to be 0.10 eV and 93 K, these values being very close to those in $Ba_{0.7}Na_{0.3}Ti_{0.7}Nb_{0.3}O_3$, which is one of the typical relaxors [22]. At $x = 4/8$, $E_a = 0.04$ eV and $T_f = 39$ K, which are rather low because the anomaly shows up at a lower temperature.

All of these observations strongly indicate that the compounds at $x = 3/8$ and $4/8$ are relaxor ferroelectrics [4–6].

4.4. Relation of T_m and ionic mass at the A site

Figure 8 plots the normalized values, $T_m(x)/T_m(0)$ and $(M(x) - M_0)/(M(0) - M_0)$, against x, where $T_m(x)$ and $M(x)$ are T_m and M at x, $T_m(0)$ and $M(0)$ being 403 K and 137.33 au [23]. The normalization as to the ionic mass at the A site employs M_0 because this is the critical

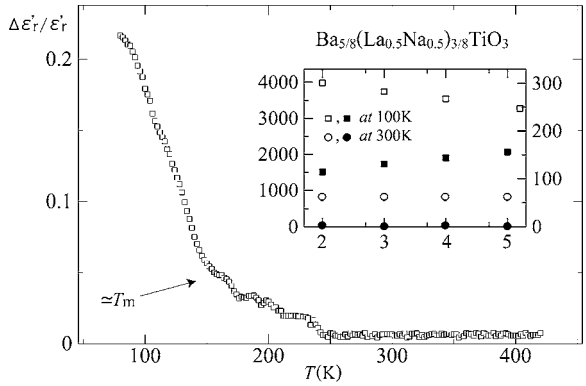

Figure 7. Temperature dependence of $\Delta\varepsilon_r'/\varepsilon_r'$ for $x = 3/8$. Inset is the frequency dependence of ε_r' (□ and ○) and ε_r'' (■ and ●) at 100 and 300 K.

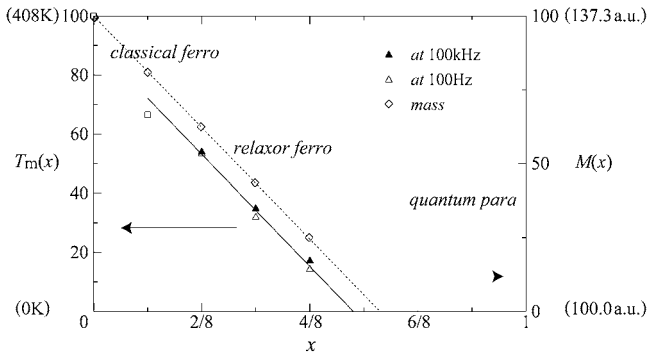

Figure 8. $T_m(x)$ and $M(x)$ versus x. The solid line represents the linear relation between $T_m(x)$ and x whereas broken line is the relation of $M(x)$ and x.

mass in the ferroelectric–paraelectric transition as described in the introduction. Two parallel relations in figure 8 are indicative of a strong correlation between $T_m(x)$ and $M(x)$. At $x \cong 5/8$, T_m reduces to 0 K and M becomes M_0. This fact involves two possibilities in the $Ba_{1-x}(La_{0.5}Na_{0.5})_xTiO_3$ system. One is that the relaxor ferroelectric–quantum paraelectric transition would take place at $x \cong 5/8$. Another one is that the quantum paraelectric at $x \geqslant 5/8$ would have no anomaly, just like $La_{0.5}Na_{0.5}TiO_3$ ($x = 1$) [20]. Such speculation suggests that the ionic mass on the A site dominates the phase transition at $x \geqslant 3/8$ in the present system.

4.5. Reduction of maximum permittivity

The non-relaxor classical ferroelectric–relaxor ferroelectric transition decreases the maximum of ε_r', i.e. a reduction of ∼70% with x increasing from 1/8 to 4/8. If based upon the assumption that $BaTiO_3$ is predominantly responsible for this reduction, a simple sum rule estimates a reduction of about 40%. There must be several reasons for such an unexpected huge reduction. As x increases, the lattice constant decreases linearly with the decrease in the ionic radius at the A site (see table 1). The displacement of Ti^{4+} suppressed by the shrinkage of the lattice constant would reduce the permittivity in a similar way to $Ba_{1-x}Na_xTi_{1-x}Nb_xO_3$, in which

the relative ratio of the ionic radius of Nb^{5+} to the lattice constant is large compared with Ti^{4+} in most perovskite titanates [22]. This suppression is likely to account for the decay of the maximum permittivity when x is small such as $2/8$. It appears necessary, however, to take into account polar nanoclusters, glass phases [10, 11] or random field [12, 24], which are indispensable for the origin of relaxors when $x = 3/8$ and $4/8$.

In most relaxor ferroelectrics, formation of polar nanoclusters and domains has been observed [25–27]. Since similar formation is expected in the present system, Ba^{2+}-rich polar clusters and La^{3+} or Na^{+}-rich domains would be formed on the analogy of B-site substituted relaxors or doped quantum paraelectrics, implying inhomogeneity to be introduced by A-site substitutions. The potentials disordered remarkably by this inhomogeneity result in random fields that stabilize the glass [24]. This glass is one of the main factors which bring about the classical ferroelectric–relaxor ferroelectric transition and this glass is also one of the important factors that decrease the dielectric permittivity at high frequencies [28]. Moreover the displacement of Ti^{4+} becomes diffusive because of the random fields, and then the maximum of ε_r' may reduce. Consequently there is the concomitant emergence of the remarkable decay in the maximum permittivity and the non-relaxor–relaxor transition when x increases.

5. Conclusion

Since A-site substitution is expected to affect crucially phase transitions in barium titanates on the analogy of B-site substitution, polycrystalline ceramic $Ba_{1-x}(La_{0.5}Na_{0.5})_xTiO_3$ specimens ($x = 1/8$–$4/8$) were prepared and the dielectric permittivity was measured against temperature up to 400 K with a frequency of 100 Hz to 100 kHz as a parametric function of x. The transition from a classical non-relaxor ferrolectric ($x = 1/8$) to a relaxor ferroelectric ($x \geqslant 3/8$) takes place, through the intermediate between non-relaxor and relaxor ferroelectrics at $x = 2/8$. The ionic mass at the A site M is found to be one of the very important parameters that govern dielectric permittivity and phase transitions. There is a strong correlation between M and the temperature of the permittivity maximum. Such a correlation includes the possibilities that there would be a relaxor ferroelectric–quantum paraelectric transition at $x \cong 5/8$ in the $Ba_{1-x}(La_{0.5}Na_{0.5})_xTiO_3$ system, $M_0 = 100$ au would be the critical mass in this transition and there would be no dielectric anomaly at $x \geqslant 5/8$. There is a huge reduction of the maximum permittivity with increasing x. The shrinkage of the lattice constant with increasing x suppresses the displacement of Ti^{4+}. Though this suppression accounts for the reduction of the maximum permittivity at $x \leqslant 2/8$, the composition at $x \geqslant 3/8$ requires further the diffusive displacement of Ti^{4+} due to the random fields created by inhomogeneity which A-site substitution introduces because the reduction of the maximum permittivity is bigger than that expected from a simple sum rule.

Acknowledgments

The authors are very grateful to H Wakai for useful advice and discussion. This work was supported by Takahashi Industrial and Economic Research Foundation.

References

[1] Berlincourt D A and Kulesar F 1952 *J. Acoust. Soc. Am.* **24** 709
[2] Kisaka S, Ikegami S and Sasaki H 1959 *J. Phys. Soc. Japan* **14** 1680
[3] Mitsui T and Westphal W B 1961 *Phys. Rev.* **124** 1354
[4] Smolenskii G A 1970 *J. Phys. Soc. Japan* **28** Suppl. 26

[5] Malibert C, Kiat J M, Durand D, Bérar J F and Spasojevic-de Biré A 1997 *J. Phys.: Condens. Matter* **9** 7485
[6] Chu F, Setter N and Tagantsev A K 1993 *J. Appl. Phys.* **77** 5129
[7] Ravez J and Simon A 1997 *Eur. J. Solid State Inorg. Chem.* **34** 1199
[8] Isupov V A 1989 *Ferroelectrics* **90** 113
[9] Yao X, Chen Z L and Cross L E 1984 *J. Appl. Phys.* **54** 3399
[10] Cross L E 1987 *Ferroelectrics* **76** 241
[11] Viehland D, Jang S J, Cross L E and Wuttig M 1990 *J. Appl. Phys.* **68** 847
[12] Westphal V, Kleemann W and Glinchuk M D 1992 *Phys. Rev. Lett.* **68** 847
[13] Sun P H, Nakamura T, Shan Y J, Inaguma Y and Itoh M 1997 *Ferroelectrics* **200** 93
[14] Shan Y J, Nakamura T, Inaguma Y and Itoh M 1998 *Solid State Ion.* **108** 123
[15] Nakamura T, Shan Y J, Sun P H, Inaguma Y and Itoh M 1998 *Ferroelectrics* **219** 71
[16] Sciau Ph, Galvarin G and Ravez J 2000 *Solid State Commun.* **113** 77
[17] Ravez J, Broustera C and Simon A 1999 *J. Mater. Chem.* **9** 1609
[18] Bednorz J G and Müller K A 1984 *Phys. Rev. Lett.* **52** 2289
[19] Prosandeev S A, Kleemann W and Dec J 2001 *J. Phys.: Condens. Matter* **13** 5957
[20] Inaguma Y, Shon J H, Kim I S, Itoh M and Nakamura T 1992 *J. Phys. Soc. Japan* **61** 3831
[21] Shannon R D 1976 *Acta Crystallogr.* A **32** 751
[22] Khemakhem H, Simon A, Von Der Muhll R and Ravez J 2000 *J. Phys.: Condens. Matter* **12** 5951
[23] Subarao E C 1973 *Ferroelectrics* **5** 267
[24] Glinchuk M D and Farhi R 1996 *J. Phys.: Condens. Matter* **8** 6985
[25] Bursill L A and Lin P J 1986 *Phil. Mag.* B **54** 157
[26] Huang W H and Vieland D 1995 *Phil. Mag.* A **71** 219
[27] Yoshida M, Mori S, Yamamoto N, Uesu Y and Kiat J M 1998 *J. Kor. Phys. Soc.* **32** S993
[28] Liu Z R, Zhang Y, Gu B L and Zhang X W 2001 *J. Phys.: Condens. Matter* **13** 1133